ABUAD Journal of Engineering Research and Development (AJERD)
ISSN (online): 2645-2685; ISSN (print): 2756-6811

Volume 7, Issue 2, 270-276

Appraisal of the Flooding Behaviour of Rotating Packed Beds

Usman GARBA[1,2], David ROUZINEAU[2], Michel MEYER[2]

[1]*Faculty of Engineering and Environmental Design, Usmanu Danfodiyo University Sokoto, Nigeria*
[2]*Chemical Engineering Laboratory, University of Toulouse, CNRS, INPT, UPS, Toulouse, France*
usman.garba@udusok.edu.ng/david.rouzineau@ensiacet.fr/
michel.meyer@ensiacet.fr

Corresponding Author: usman.garba@udusok.edu.ng, +2347064436033
Date Submitted: 06/05/2024
Date Accepted: 04/09/2024
Date Published: 14/09/2024

Abstract*: Rotating packed beds (RPBs) enhances mass transfer processes because a centrifugal force which is several -times greater than gravity is used as the driving force. The complexity of fluid flow across RPBs has made predicting and accurately determining their hydrodynamic behaviours difficult. The flooding point as a hydrodynamic characteristic is essential for the accurate design and scale-up of RPBs. However, variations in flooding point definitions and methodologies across the literature highlight the need for standardized approaches in studying RPB flooding phenomena. This study compared four approaches based on pressure drop fluctuations and the volume of liquid ejected from the RPB to determine the onset of flooding in RPBs using experimental results from a pilot-scale counter-current RPB. For rotational speeds of 300 -1500 rpm, gas flow rate of 100-300 Nm^3/h, and liquid flow rates of 0.39-0.75 m^3/h, the pressure drop varied from 314 to 2,100 Pa. Quantitative comparisons of the results based on different flooding point definitions showed wide variations with the values of the pressure drop at the onset of flooding differing by as much as 325 %. A quantitative approach based on virtual observations and the ejection of 8 % of the total liquid flow rate from the rotor's eye is proposed as the standard method for identifying the onset of flooding in RPBs.*

Keywords: *Flooding, Flooding Point, Rotating Packed Beds, Pressure Drop, RPB Flooding Curves*

1. INTRODUCTION

Understanding the hydrodynamic principles is crucial in designing, modelling, and scaling up. It is essential to obtain fundamental data for developing rules and guidelines for designing and controlling newer separation equipment such as rotating packed beds (RPB). The RPB is an innovative process intensification equipment that utilises centrifugal force as opposed to the conventional gravity used in previous separation equipment [1]–[3].

As gas-liquid contacting devices, the centrifugal force in RPBs greatly enhances the interphase contact area and consequently, mass transfer efficiency, by shredding the liquid flow into films, filaments, and droplets as determined by the rotation speed of the rotor [4], [5]. Like conventional packed separation columns, hydrodynamic characteristics such as the loading point and the flooding point are essential in RPB operations. Various RPB hydrodynamic parameters such as liquid holdup, gas pressure drop, liquid dispersion, and flooding are extensively discussed in the literature [6], [7]. Accurately predicting pressure drops and upper operating limits is key to understanding essential aspects of RPB hydrodynamics. Despite significant research and industrial applications, the design of RPBs remains case-specific and in need of improvement [1], [7], [8]. In conventional packed separation columns, flooding occurs when the liquid flow surpasses the packing material's capacity for gas-liquid contact, leading to ineffective mass transfer. Determining flooding points is critical for safe and economical operations. Numerous studies have explored the influence of pressure drop in RPBs using empirical models and measurement techniques such as the fractionation method, visual studies, the use of Doppler optical probes, and the use of artificial neural networks [9]–[12]. RPBs typically exhibit higher hydraulic capacities, pressure drops, and flooding capacities compared to conventional packed separation columns (CPSCs), allowing for the use of high-porosity packings and specific surface areas. This enables RPBs to utilize high-porosity packings of up to 90 to 95% and high specific surface areas in the range of 2000 to 5000 m^2/m^3 [7], [13], [14]. However, identifying design factors like loading and flooding points is more challenging in RPBs due to the complexity introduced by rotation. In RPB operations, two-phase flows are common, including gas and liquid. Dhaneesh & Ranganathan [15] reported that due to the strong centrifugal acceleration in RPBs, packings with high contact areas are used allowing for the utilization of the reactor at high flooding limits.

The presence of liquid in RPB packing reduces available area and increases frictional pressure drop. Different methods for characterizing flooding in RPBs have been proposed, including visual observations and pressure drop fluctuation methods. Various approaches exist for determining flooding points in RPBs [16], each with its advantages and limitations. Rao *et al.*, [17] reported that flooding in RPBs (otherwise referred to as the upper operating limit) differs from that in

CPSCs because of the doughnut shape of the flow area, the presence of the centrifugal field, and the orientation of the rotor. Additionally, for RPBs, the entire rotor does not get flooded, and the holdup does not increase steeply. According to Neumann *et al.*, [18], the flooding in RPBs, occurs in the 'eye' of the rotor because it has the lowest centrifugal field and the highest mass fluxes. Hence, Hendry *et al.* [7] explained that the pressure drops during flooding in RPBs are inconsistent because the flooding is accompanied by liquid rejection from the eye of the rotor. In RPB operations, the most common multiphase flows are the two-phase flows which include gas-liquid flow and, liquid-liquid flows. The presence of a liquid in an RPB packing is perceived to serve as an extra liquid film which reduces the available area of the packing. The lowered free area of the packing consequently leads to an increase in the frictional pressure drop [19]. Thus, many researchers ([7], [20]) hypothesized that the presence of a liquid increases the opposition of the gas flow by blocking some of the packing pores and thus reducing the porosity of the packing which leads to an increase in pressure drop. An analysis of previous literature has shown several different methods and approaches (both visual and calculation) for characterizing flooding in RPBs. The first method is the use of observing the onset of the splash of the liquid in the eye of the rotor [8]. The procedure involves neutralizing two operating variables (rotation speed, liquid flow rate for example) and manipulating the third one (varying gas flow rate). If the gas flow rate increases beyond the flooding point, the liquid will accumulate in the center of the rotor. The second method is the use of the pressure drop fluctuation method [21]–[23]. In this method, the RPB flooding points are inferred from the total pressure drop polynomial curve against angular velocity at constant gas and liquid flow rates. The procedure is similar to that of the first method described above. However, in this method, the approach is to begin with a high rotation speed and then reduce it gradually until the flooding point is reached [22]. Hendry *et al.*, [7] used a slightly different variation of this method by identifying the flooding point as a fast increase in ejected liquid on decreasing the rotation speed. Flooding was considered to start when the flow rate of ejected liquid through the gas outlet was up to 8% of the total inlet flow rate. The procedure of Hendry *et al.* [7] introduced a more quantitative approach to the determination of the onset of flooding in RPB operations. However, the approach may not be feasible when dealing with expensive or toxic fluids. In the third method, a combination of the two methods mentioned above is adopted. The flooding point is identified by increasing the gas flow rate and, in another set of experiments, by decreasing the rotation speed. In both cases, the flooding point is determined by the physical observation of the liquid entrainment occurring in the eye and the use of the pressure drop curve [8]. Finally, in the fourth approach by Burns et al., [6], the variation in the liquid holdup without and with the gas flow in the RPB was used to determine the flooding point. Flooding was taken as when the ratio of liquid holdup without gas flow to the liquid holdup with gas flow diverges from 1. Based on the various approaches and methods of obtaining the flooding points of RPBs as discussed above, [17], [24] highlighted that there exist various definitions of the flooding point for RPBs. Hendry *et al.*, [7] and Neumann, *et al.*, [8] reported inconsistencies in the literature on the methods adopted to determine the beginning of flooding in RPBs. Several divergent definitions have been given by various researchers for the RPB flooding phenomena [7], [21]–[23], [25]. Table 1 is a compilation of some definitions of the flooding point in RPBs as presented in some previous literature.

Table 1: Different definitions of RPB flooding points

s/No.	Various Flooding definition	References
(i)	The point where the value of the slope of the plot of logarithmic pressure drops against the logarithmic gas flow rate is ≥ 2.	[26]
(ii)	A step increase in pressure drop amounting to 5 Pa per unit decreases rotation speed as measured per minute.	[22]
(iii)	The point where the pressure drop across the RPB increases to a maximum then abruptly begins to fall.	[21]
(iv)	The point of minimum pressure drop in the pressure drops against rotation speed polynomial curve.	[23]
(v)	The point where the expelled liquid flow rate suddenly exceeds 8 % of the inlet liquid flow rate.	[7]

Pressure drop serves as a critical indicator for assessing the energy consumption and resistance within Rotating Packed Beds (RPBs). Higher pressure drops signify increased fluid flow and consequently higher energy consumption. Therefore, various aspects of RPBs, including structural design, capacity, selection of internals, and operational costs, are all interconnected with energy requirements dictated by the pressure drop. Figure 1(a) illustrates a typical RPB pressure drop profile against the rotor speed, delineating flooding definitions according to multiple authors. For instance, Gładyszewski et al.,[27] demonstrated that layers of anisotropic packings made of rings made from chrome-nickel foams of various specific surface areas ranging from 500 to 2800 m^2/m^3 and porosity of 92 % operated in a countercurrent RPB with an outer casing radius of 230 mm, an inner rotor diameter of 73 mm and an outer rotor diameter of 200 mm, exhibited the depicted characteristic curve. Similarly, numerous other studies have documented analogous pressure drop profiles against rotor speed for RPBs [8], [17]. By comparing three-dimensional packings with pall rings and wire mesh packings in RPBs, Yuan *et al.* [28] showed that the three-dimensional packings produced expressively lower the pressure drops, which underscores the dependence of the flooding in RPBs on the packing characteristics.

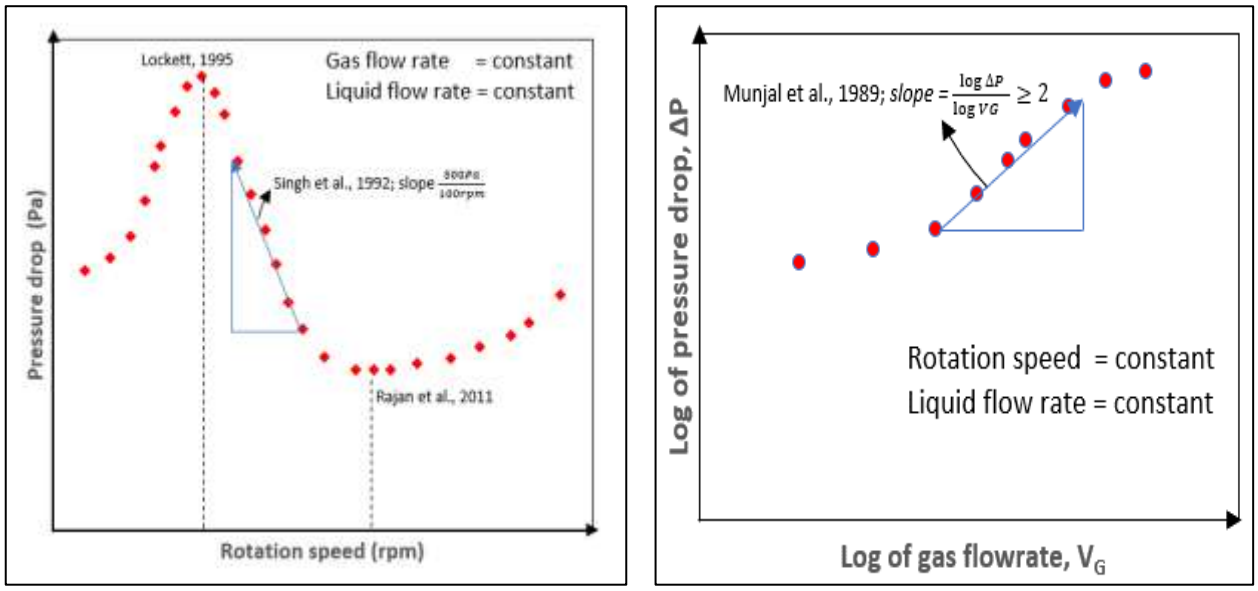

Figure 1: A schematic of the definitions of RPB flooding as given by various literature sources

Comprehensive studies that compared the different definitions of RPB flooding towards establishing standard criterion and definition for the phenomenon are scarce in the literature. This study compares experimental values of the RPB flooding point based on four reported definitions of RPB flooding. The goal is to identify a standard for this crucial RPB design parameter by evaluating the strengths and weaknesses of each definition. This comparison aims to provide a foundation for determining the most accurate option and establishing a consistent method for identifying flooding limits in RPBs.

2. METHODOLOGY

A pilot-scale RPB (RPB500) from Proceller, Poland, was used to facilitate a counter-current air-water flow system under ambient conditions. The RPB rotor, with inner and outer radii of 80 mm and 250 mm respectively, and an axial height of 40 mm, employed a commercial structured packing element made of stainless steel. The packing had a total area per unit volume of 2400 m^{-1}, a porosity of 86%, and an axial height of 40 mm. Water, stored in a 0.6 m^3 polypropylene tank, was supplied to the RPB via a magnetic drive pump (Iwaki, model MDG-R15P), distributed through a single central liquid distributor with 32 holes each 1.5 mm in diameter. The liquid flow rate was regulated by a ball valve and measured with a liquid flow meter (Brooks Instruments, Model 2510). Ambient air, provided by a single-stage side channel blower (BUTSCH SAMOS, SB 0430 D0), with a nominal pumping speed of 500 m^3/h and a maximum differential pressure of 260 mbar, was measured using a calibrated variable area flow meter (Brooks, MT3809 Series). The pressure drop across the RPB was gauged using a differential pressure sensor (Rosemount 3051 Pressure Transmitter).

2.2 Experimental Procedure

During each experiment, three process parameters were varied within specific ranges: rotational speed (300-1500 rpm), gas flow rate (100-300 Nm^3/h), and liquid flow rate (0.39-0.75 m^3/h). Two methods were employed to monitor RPB flooding points. The first method, inspired by [8] and [28], involved observing the pressure drop while varying one process parameter while keeping the other two constant, identifying flooding onset when the first droplets appeared at the liquid outlet. The second method, based on the quantitative approach of Hendry [3] and Garba et al. [25], observed increasing acceleration of liquid droplets with rotational speed, leading to fast liquid ejection from the rotor's eye to the gas outlet. Liquid ejection was collected using a hydrocyclone attached to the gas outlet, with flooding onset determined when the volume of ejected liquid exceeded 8% of the total liquid flow into the RPB. Each experimental run was repeated at least three times to ensure reproducibility.

3. RESULTS AND DISCUSSION

3.1 RPB Flooding Point as Determined by Pressure drop Variations

Pressure measurements and the effect of rotation speed on wet pressure drop were plotted and presented in Figure 2. The characteristic pressure drop curve of RPBs was consistently observed across all the combinations of operating conditions studied. At constant gas and liquid flow rates, a rapid pressure drop decrease was observed as rotation speed decreased from the maximum of 1400 rpm, with a decrease of about 28% per 200 rpm decrease in speed. Conversely, at constant rotation speed and liquid flow rate, a 35% average pressure drop increase was observed for each 50 Nm^3/h gas flow rate increase. Generally, rotation speeds below 600 rpm yielded a rapid decrease in pressure drop, while speeds above

600 rpm led to a rapid increase. The decrease in pressure drop with decreasing rotation speed was attributed to a reduced need for overcoming rotation-induced pressure drop and decreased forced rotation of air in the rotor. A minimum pressure drop was reached at 600 to 400 rpm, beyond which only very small pressure drop changes were observed. Increases in pressure drops at lower rotational speeds were linked to increased liquid holdup, film thickness, liquid entrainment, and flooding, potentially blocking packing pores and increasing gas velocity, resulting in frictional pressure drop. (Burns et al. [6] explained this phenomenon as a consequence of increased liquid holdup and film thickness with reduced rotational speed of the rotor, which leads to less free space in the packing which increases the pressure drop. Conversely, at lower speeds, liquid accumulation and flooding increased pressure drop. Conversely, at lower rotational speeds greater than 400 rpm, two main factors contribute to the increased pressure drop: increased liquid entrainment, and flooding. The accumulation of liquid can potentially block the packing pores, reducing the cross-sectional area for flow and increasing gas velocity, resulting in a frictional pressure drop in the packing.

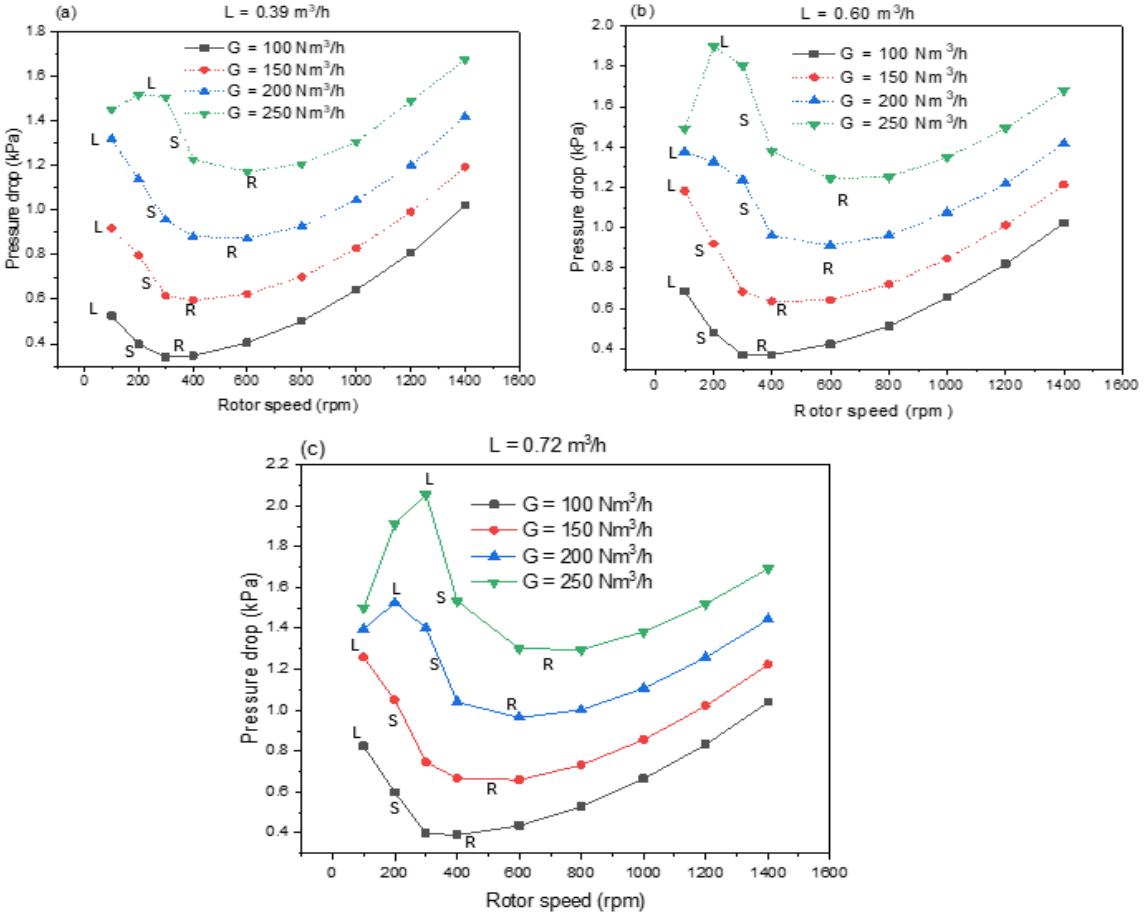

Figure 2: Effect of rotor speed on pressure drop at gas varying gas flow rates from 100 to 250 Nm^3/h for (a) L= 0.39 m^3/h (b) L= 0.6 m^3/h (c) L= 0.72 m^3/h indicating points of RPB flooding according to the definitions of Lockett [21], Singh *et al.*, [22] and, Rajan *et al.*, [23]

Figure 2 illustrates that increasing either gas or liquid flow rate at a constant rotation speed results in a higher pressure drop. Elevating the gas flow rate heightens pressure drop due to friction with packing components, gas compression, and pressure gradient-induced changes in the gas flow direction. Similarly, augmented liquid flow rates raise pressure drop by blocking packing pores, inducing inertial Coriolis forces on the moving gas within the packing, forming regions where gas rotates along a straight or curved axis (free vortices), and accumulating liquid in the rotor's eye.
Three distinct definitions of RPB flooding proposed by [21], [22], and, [23] were employed to determine the pressure drop at flooding (refer to Figure 2). A comparison of these definitions revealed significant disparities in values of the pressure drop at flooding, ranging from 12% to 59%. This indicates that unlike in conventional separation columns, pressure drop readings alone are insufficient indicators of flooding points in RPBs.

3.2 RPB Flooding Point as Determined by the Quantity of Ejected Liquid

Figure 3 presents contour plots of flooding experiments based on the methodology of [7], showing plots for the lowest and highest liquid flow rates utilized. Flooding, defined as liquid entrainment equal to or exceeding 8% of the total liquid inlet flow rate, is depicted in red-shaded regions on the contour plots, while blue-shaded areas represent operational regions without flooding or liquid entrainment. The shading intensity indicates the percentage of flooding. The boundary

between colours represents loading points, where the gas pressure gradient from the outer packing counteracts the liquid force from the inner packing, often characterized by a visible liquid accumulation in the RPB eye. At constant gas and liquid flow rates, flooding in packed separation columns initiates due to instability arising from the interaction between pressure gradient, liquid holdup, and wave-type instability. Consequently, across all liquid flow rates studied, low rotation speeds lead to flooding due to low centrifugal forces, governed by gas flow rate and liquid instability in the rotor's eye. At a low liquid flow rate of 0.39 m^3/h, flooding occurs at low rotation speeds (<200 rpm) and medium to high rotation speeds (900-1400 rpm) for a relatively high gas flow rate range of 160-250 Nm^3/h. Conversely, at higher liquid flow rates of 0.6 and 0.72 m^3/h, flooding occurs at the same low rotation speed range but at a lower gas flow rate of approximately 115 Nm^3/h. Additionally, no flooding is observed at the two higher liquid flow rates when operated at rotation speeds exceeding 300 rpm across all gas flow rate ranges.

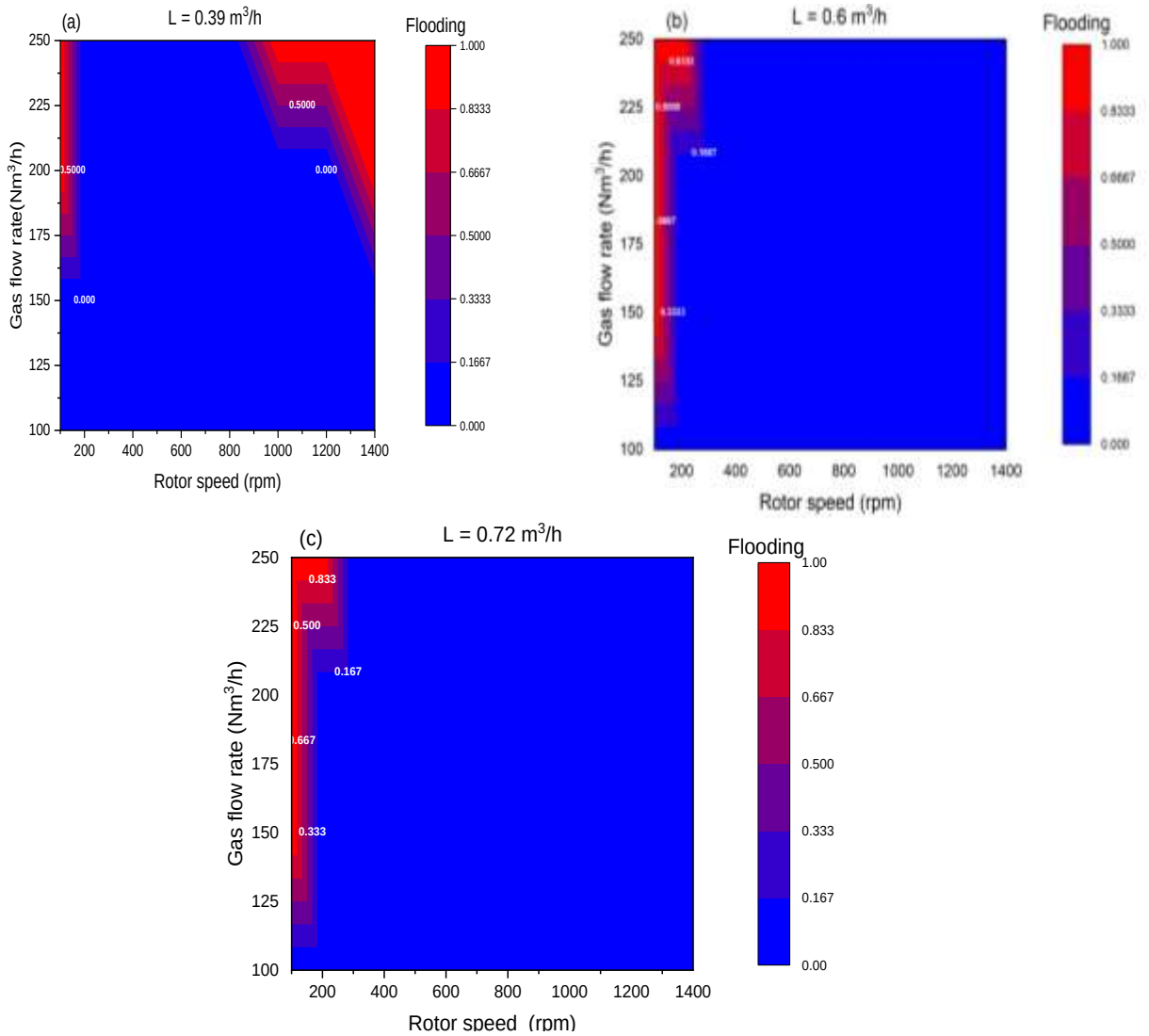

Figure 3: Contour plots showing combination of operating conditions at which flooding is absent (blue coloured area), and operating conditions at which flooding and entrainment are recorded (red coloured area) for various liquid flow rates

Figures 3 (a) and (b) illustrate the minimal impact of liquid flow rate on RPB pressure drop. Transitioning from 0.6 to 0.72 m^3/h resulted in nearly identical contour plots, with the pressure drop difference between these two conditions being less than 10%. Li *et al.* [29] emphasized that increased pressure drop is primarily attributed to packing surface drenching and liquid obstructing packing pores to gas flow. Hence, RPB pressure drop correlates with rotation speed and gas flow rate, underscoring the marginal influence of liquid flow rates.

3.3 Comparison of Pressure Drop at RPB Flooding Point across Different Definitions

At a low liquid flow rate of 0.39 m^3/h and a high gas flow rate of 250 Nm^3/h, which induced flooding at both low and high rotation speeds, Table 2 presents a comparison of pressure drop values at the onset of flooding, as obtained using

various definitions depicted in Figure 2. Pressure drop values based on the RPB flooding definition by Rajan *et al.* [23], relying on minimum pressure drop, are utilized for the comparisons.

Table 2: Comparison of pressure drop at the onset of RPB flooding as obtained based on various definitions

References	Pressure drop at the onset of flooding (kPa)	Deviation from minimum (%)
[22]	0.526	54
[21]	0.399	17
[23]	0.341	-
[7]	1.449	325

Table 2 demonstrates notable discrepancies in pressure drop at flooding, spanning from 17% to 325%. The highest pressure drop was recorded following the methodology outlined in Hendry *et al.* [7]. The observation was caused by the increased liquid accumulation within packing pores and the rotor eye. These variations underscore the limitations of relying solely on pressure drop as a predictor of flooding points in RPBs, as advocated by some researchers. The intricate fluid flow dynamics through RPB packings contribute to these disparities. Thus, employing a qualitative approach, which considers visual inspection of liquid retention in the rotor eye, liquid holdup in the packing, and liquid ejection from the gas outlet, emerges as a more dependable method for determining RPB flooding points. While qualitative assessments suffice for most cases, incorporating gas pressure measurements serves as a supplementary safety measure, especially when dealing with hazardous or expensive fluids. The gas pressure measurement in such a method is needed to serve as a guide and for safety purposes. However as observed by Garba *et al.* [30], the use of such a method to obtain RPB flooding points may be challenging when toxic or costly fluids are involved.

4. CONCLUSION

This study rigorously investigated flooding behavior, a fundamental hydrodynamic aspect of RPBs, by examining the influence of key operational parameters. The influence of the three major operating parameters of the RPB was explored. Two of the most commonly used approaches to determine flooding in RPBs were used to ascertain the pressure drop variations and consequently, the onset of flooding. For process parameters covering a rotational speed of 300-1500 rpm, gas flow rate of 100-300 Nm^3/h, and a liquid flow rate of 0.39-0.75m^3/h, the pressure drop varied from 314 to 2,100 Pa. A wide variation in the values of the pressure drop at the onset of flooding was as high as 325%. A quantitative approach based on both virtual observations and the ejection of 8 % of the total liquid flow rate from the eye of the rotor is proposed as the standard method of identifying the onset of flooding in RPBs. The proposed method complements visual observations and pressure drop measurements

REFERENCES

[1] Wojtasik-Malinowska, J., Jaskulski, M. & Jaskulski, M. (2022). CFD Simulation of Gas Pressure Drop in Porous Packing for Rotating Packed Beds (RPB) CO_2 Absorbers, *Environ. Sci. Pollut. Res.*, 29, 71857–71870. https://doi:10.1007/S11356-022-20859-X .

[2] Ayash, M. A. & Mahmood, A. A. (2022). Conventional and Non-Conventional Gas-Liquid Contacting Methods: A Critical Review and a Quantitative Evaluation. *AIP Conf. Proc.*, 2660(020073), 1-22. https://doi:doi:10.1063/5.010772

[3] Shukla, C., Mishra, P. & Dash, S. K. (2023). A Review of Process Intensified CO_2 Capture in RPB for Sustainability and Contribution to Industrial Net Zero. *Front. Energy Res*., 11, 1-17. https://doi:10.3389/fenrg.2023.1135188.

[4] Tian, W., Ji, J., Li, H., Liu, C., Song, L., Ma, K., Tang, S., Zhong, S., Yue, H. & Liang. B. (2022). Measurements of the Effective Mass Transfer Areas for the Gas–Liquid Rotating Packed Bed. *Chinese J. Chem. Eng.*, 55, 13–19. https://doi:10.1016/j.cjche.2022.06.002.

[5] Liu, J.F., Luo, Y., Chu, Y., Larachi, G.-W., Zou, F. & Chen, H.K. (2020). Liquid Microflow Inside the Packing of a Rotating Packed Bed Reactor: Computational, Observational and Experimental Studies. *Chem. Eng. J.*, 386(xxx), 1-14. https://doi.org/10.1016/j.cej.2019.03.010.

[6] Burns, J. R., Jamil, J. N. & Ramshaw, C. (2000). Process Intensification: Operating Characteristics of Rotating Packed Beds - Determination of Liquid Hold-Up for a High-Voidage Structured Packing. *Chem. Eng. Sci.*, 55, 2401–2415. https://doi:10.1016/S0009-2509(99)00520-5.

[7] Hendry, J. R., Lee, J. G. M. & Attidekou, P. S. (2020). Pressure Drop and Flooding in Rotating Packed Beds. *Chem. Eng. Process. - Process Intensif.*, 151(107908), 1-7. https://doi:10.1016/j.cep.2020.107908 .

[8] Neumann, K., Hunold, S., Groß, K. & Górak, A. (2017). Experimental Investigations on the Upper Operating Limit in Rotating Packed Beds. *Chem. Eng. Process. Process Intensif.*,121, 240–247. https://doi:10.1016/j.cep.2017.09.003.

[9] Han-Zhuo, J.F.C., Liu, X. Z., Li, Y.B., Zhang, L. L. & Chu, G. W. (2024). Liquid Dispersion Behaviors in a Rotating Packed Bed with Different Packing Arrangements: A Comparison Study. *Chem. Eng. Sci.*, 293(2024), 120054. https://doi.org/10.1016/j.ces.2024.120054.

[10] Alatyar, A. M. & Berrouk, A. S. (2023). Hydrodynamic Behavior Of Liquid Flow in a Rotating Packed Bed. *Chem. Eng. Res. Des.*, 197, 851–870. https://doi:10.1016/j.cherd.2023.08.032.

[11] Liu, Y., Luo, Y., Chu, G. W., Larachi, F., Zou, H. K. & Chen, J. F. (2020). Liquid Microflow Inside the Packing of a Rotating Packed Bed Reactor: Computational, Observational And Experimental Studies. *Chem. Eng. J*., 386, 1–14. https://doi:10.1016/j.cej.2019.03.010.

[12] Wen, Z.N., Li, Y.B., Xu, H. Z., Xu, Y.C., Sun, C., Zou, H. K., Chu, G.W. (2023). Liquid Flow Behavior in the Concentric Mesh Packing With Novel Fiber Cross-Sectional Shape in a Rotating Packed Bed, *Chemical Engineering Journal.*, 451(4), 1385-8947. https://doi.org/10.1016/j.cej.2022.139094.

[13] Ghadyanlou, F., Azari, A. & Vatani, A. (2021). A Review of Modeling Rotating Packed Beds and Improving their Parameters: Gas–Liquid Contact. *Sustainability*., 13(8046), 1-42. https://doi.org/10.3390/su13148046.

[14] Lin, C. & Liu, W. (2017). Mass Transfer Characteristics of a High-voidage Rotating Packed Bed, *J. Ind. Eng. Chem*., 13(1), 71-78.

[15] Dhaneesh, K. P. & Ranganathan, P. (2022). A Comprehensive Review on the Hydrodynamics, Mass Transfer and Chemical Absorption of CO_2 and Modelling Aspects of Rotating Packed Bed. *Sep. Purif. Technol.*, 295, 121248. https://doi:10.1016/j. seppur.2022.121248.

[16] Zheng, C., Guo, K., Feng, Y.,Yang, C. & Gardner, N. C. (2000). Pressure Drop of Centripetal Gas Flow through Rotating Beds. *Ind. Eng. Chem. Res.*, 39(3), 829–834. https://doi:10.1021/ie980703d.

[17] Rao, D. P., Bhowal, A. & Goswami, P. S. (2004). Process Intensification in Rotating Packed Beds (HIGEE): An Appraisal. *Ind. Eng. Chem. Res.*, 43(4), 1150–1162. https://doi:10.1021/ie030630k.

[18] Neumann, K., Hunold, S., Skiborowski, M. & Górak, A. (2017). Dry Pressure Drop in Rotating Packed Beds - Systematic Experimental Studies. *Ind. Eng. Chem. Res.*, 56(4), 12395–12405. https://doi:10.1021/acs.iecr.7b03203.

[19] Guo, F., Zheng, C., Guo, K., Feng, Y. & Gardner, N. C. (1997). Hydrodynamics and Mass Transfer in Cross-Flow Rotating Packed Bed. *Chem. Eng. Sci.* 52(21–22), 3853–3859. https://doi:10.1016/S0009-2509(97)00229-7.

[20] Sandilya, P., Rao, D. P., Sharma, A. & Biswas, G. (2001). Gas-Phase Mass Transfer in a Centrifugal Contactor. *Ind. Eng. Chem. Res.*, 40(1), 384–392. https://doi:10.1021/ie0000818.

[21] Lockett, M. J. (1995). Flooding of Rotating Structured Packing and its Application to Conventional Packed Columns, *Chem. Eng. Res. Des*. 73, 379–384.

[22] Singh, S. P., Wilson, J.H., Counce, R. M., Villiers-Fisher, J. F. & Jennings, H. L. (1992). Removal of Volatile Organic Compounds from Groundwater using a Rotary Air Stripper. *Ind. Eng. Chem. Res*. 31(2), 574–580. https://doi:10.1021/ie00002a019.

[23] Rajan, S., Kumar, M., Ansari, M. J., Rao, D. P. & Kaistha, N. (2011). Limiting Gas Liquid Flows and Mass Transfer in a Novel Rotating Packed Bed (HiGee). *Ind. Eng. Chem. Res.*, 50(2), 986–997. https://doi:10.1021/ie100899r.

[24] Groß, K., Neumann, K., Skiborowski, M. & Górak, A. (2018). Analysing the Operating Limits in High Gravity Equipment. *Chem. Eng. Trans.*, 69, 661–666. https://doi:10.3303/CET1869111.

[25] Munjal, S., Dudukovć, M. P. & Ramachandran, P. (1989). Mass-Transfer in Rotating Packed Beds-I. Development of Gas-Liquid and Liquid-Solid Mass-Transfer Correlations. *Chem. Eng. Sci.*, 44(10), 2245–2256. https://doi:10.1016/0009-2509(89)85159-0

[26] Munjal, S., Dudukovć, M. P. & Ramachandran, P. (1989). Mass-Transfer in Rotating Packed Beds-II. Experimental Results and Comparison with Theory and Gravity Flow. *Chem. Eng. Sci.*, 44(10), 2257–2268. https://doi:10.1016/0009-2509(89)85160-7.

[27] Gładyszewski K., Grob, K., Bieberle, A., Schubert, M., Hild, M., Górak, A. & Skiborowski, M. (2021). Evaluation of Performance Improvements through Application of Anisotropic Foam Packings in Rotating Packed Beds. *Chemical Engineering Science.*, 230, 1-13. https://doi.org/10.1016/j.ces.2020.116176.

[28] Yuan, Z.G., Wang, Y. X., Liu, Y. Z., Wang, D., Jiao, W.Z. & Liang, P. F. (2022). Research and Development of Advanced Structured Packing in a Rotating Packed Bed. *Chinese J. Chem. Eng.*, 49, 178–186. https://doi:10.1016/j.cjche.2021.12.023.

[29] Liu, X., Jing, M., Chen, S. & Du, L. (2018). Experimental Study of Gas Pressure Drop in Rotating Packed Bed with Rotational-Stationary Packing. *Can. J. Chem. Eng.*, 96(2), 590–596. https://doi:10.1002/cjce.22936.

[30] Garba, U. Adamu, A., Triquet, T., Rouzineau, D. & Meyer, M. (2023). Experimental Study of the Effect of Viscous Media on the Hydrodynamic Characteristics of a Rotating Packed Bed. *Chem. Eng. Process. - Process Intensif*., 191, 1-11. https://doi:10.1016/j.cep.2023.109482